



Subcascade formation in displacement cascade simulations: Implications for fusion reactor materials ¹

Roger E. Stoller ^{a,*}, Lawrence R. Greenwood ^b

^a *Metals and Ceramics Division, Oak Ridge National Laboratory, Oak Ridge, TN 37831-6376, USA*

^b *Environmental Technology Division, Pacific Northwest National Laboratory, Richland, WA 99352, USA*

Abstract

Displacement cascade formation in iron has been investigated by the method of molecular dynamics (MD) for cascade energies up to 40 keV, corresponding to PKA energies up to 61 keV. The results of these simulations have been used in the SPECOMP code to obtain effective, energy-dependent cross sections for two measures of primary damage production: (1) the number of surviving point defects expressed as a fraction of the those predicted by the standard secondary displacement model by Norgett, Robinson, and Torrens (NRT), and (2) the fraction of the surviving interstitials contained in clusters that formed during the cascade event. The primary knockon atom spectra for iron obtained from the SPECTER code have been used to weight these MD-based damage production cross sections in order to obtain spectrally averaged values for several locations in commercial fission reactors, materials test reactors, and a DT fusion reactor (ITER) first wall. An evaluation of these results indicates that neutron energy spectrum differences between the various environments do not lead to significant differences between the average primary damage formation parameters. This conclusion implies that the displacement damage component of radiation damage produced in a DT fusion reactor should be well simulated by irradiation in a fission reactor neutron spectrum, and that differences in nuclear transmutation production may be the primary source of uncertainty in the prediction of material performance at high doses in DT fusion reactors. © 1999 Elsevier Science B.V. All rights reserved.

1. Introduction

Estimates of structural material performance in first generation deuterium–tritium (DT) fusion reactors such as the ITER must be made largely on the basis of data obtained in fission reactors. A primary uncertainty in such use of the fission reactor data base is the potential impact of the higher energy neutrons that are produced by the DT reaction. For example, a typical fission re-

actor spectrum has few neutrons above 5 MeV, while a DT fusion neutron spectrum has a peak at 14.1 MeV. These neutrons will in turn lead to the production of displacement damage by higher energy primary knockon atoms (PKA) in the fusion environment. In addition, the production rates of transmutation products (notably hydrogen and helium) will be significantly higher near the first wall of a DT fusion reactor than in the high-flux fission reactor sites that are typically used in irradiation experiments [1].

The issue of PKA energy effects can be addressed through the use of displacement cascade simulations using the method of molecular dynamics (MD). Although MD simulations can provide a detailed picture of the formation and evolution of displacement cascades, they impose a substantial computational burden. However, recent advances in computing equipment permit the simulation of high energy displacement events involving more than one-million atoms [2–4]; the results presented below will encompass MD cascade simulation energies from near the displacement

* Corresponding author.: Fax: +1-423 574 0641; e-mail: rkn@ornl.gov.

¹ Research sponsored by the Office of Nuclear Regulatory Research, US Nuclear Regulatory Commission under inter-agency agreement DOE 1886-8109-8L with the US Department of Energy and by the Division of Materials Sciences, US Department of Energy under contract DE-AC05-96OR22464 with Lockheed Martin Energy Research Corporation, and the Office of Fusion Energy, US Department of Energy at the Pacific Northwest National Laboratory.

threshold to as high as 40 keV. Two parameters have been extracted from the MD simulations: the number of point defects that remain after the displacement event is completed and the fraction of the surviving interstitials that are contained in clusters. For the purpose of comparison with standard dosimetry, these values have been normalized to the number of atomic displacements calculated with the secondary displacement model by Norgett, Robinson, and Torrens (NRT) [5].

The energy dependence of the two MD defect parameters was used to evaluate the effects of neutron energy spectrum. Simple, energy-dependent functional fits to the MD results were obtained, and the SPECOMP code [6] was used to compute effective cross sections for point defect survival and point defect clustering. PKA spectra for iron obtained from SPECTER [7] were then used to weight these effective cross sections in order to calculate spectrum-averaged values for various neutron irradiation environments, including several locations in both water and sodium-moderated fission reactors, and a DT fusion reactor first wall [8].

2. MD Cascade simulations

The molecular dynamics code, MOLDY, and the interatomic potential for iron used in this study are described in detail in Refs. [9–11]. Additional details on the results obtained by this method can be found in Refs. [2–4,12]. Briefly described, the process of conducting a cascade simulation requires two steps. First, a block of atoms of the desired size is thermally equilibrated. This process permits the lattice thermal vibrations (phonon waves) to be established for the simulated temperature, and typically requires a simulation time of approximately 10 ps. This atom block can be saved and used as the starting point for several subsequent cascade simulations. Then, the cascade simulations are initiated by giving one of the atoms a defined amount of kinetic energy, E_{MD} , in a specified direction. This atom is equivalent to the PKA following a collision with a

neutron. Statistical variability can be introduced by either further equilibration of the starting block or by choosing either a different primary knockon atom or PKA direction. Typically, at least six different cascades are required to obtain results that can be used to represent the average behavior at any one energy and temperature.

The MOLDY code describes only elastic collisions between atoms; it does not account for energy loss mechanisms such as electronic excitation and ionization. Thus, the initial energy E_{MD} given to the simulated PKA is approximately equivalent to the damage energy (T_{dam}) in the NRT model [5]. Using the values of E_{MD} in Table 1, the corresponding E_{PKA} and the NRT defects in iron have been calculated using the procedure described in Ref. [5] with the recommended 40 eV displacement threshold [13]. These values are also listed in Table 1. Note that the difference between the MD simulation, or damage energy, and the PKA energy increases as the PKA energy increases [5]. For purposes of comparison, the parameters for the maximum DT neutron energy of 14.1 MeV are also included in Table 1.

It is not simple to determine whether or not the absence of electronic energy losses has a significant influence in the MD cascade simulations. For example, electron–phonon coupling could alter the rate of cascade cooling and either promote or inhibit defect clustering. However, the results of the cascade simulations have been shown to be broadly consistent with experimental observations [12], suggesting that the overall impact may not be large. Since the primary purpose of this paper is to make a relative comparison of different irradiation environments, modest changes to the parameters derived from the MD simulations should not alter the conclusions.

The cascade simulations are continued until the phase of in-cascade recombination of vacancies and interstitials is complete and the atom block has returned to near thermal equilibrium. The required time varies from about 5 ps for the low-energy cascades to 15–20 ps for the 40 keV cascades. The computing time with the

Table 1
Typical MD cascade parameters and required atom block sizes

Neutron energy (MeV)	Average PKA energy (keV)	Corresponding E_{MD} (keV)	NRT displacements	Atoms in simulation
0.00335	0.116	0.1	1	3456
0.00682	0.236	0.2	2	6750
0.0175	0.605	0.5	5	6750
0.0358	1.24	1.0	10	54 000
0.0734	2.54	2.0	20	54 000
0.191	6.6	5.0	50	128 000
0.397	13.7	10.0	100	250 000
0.832	28.8	20.0	200	250 000
1.77	61.3	40.0	400	1 024 000
14.1	487.0	220.4	2204	^a

^a No simulations done, displacement parameters included for comparison only.

MOLDY code is almost linearly proportional to the number of atoms in the simulation. Higher energy events require a larger atom block as listed in Table 1. Two to three weeks of cpu time is required to complete the highest energy 40 keV cascade simulations with 1,024,000 atoms for 15 ps on a modern high-speed workstation equipped with a MIPS R8000 cpu and 256 Mb of memory.

Two parameters are of primary interest to this work: the number of point defects that survive after in-cascade recombination is complete, and the fraction of the surviving interstitials that are contained in clusters rather than as isolated defects. The former is important because it is only the surviving point defects that can contribute to radiation-induced microstructural evolution. The latter is significant because these small clusters provide nuclei for the growth of larger defects which can give rise to mechanical property changes. The formation of these small clusters directly within the cascade means that the extended defects can evolve more quickly than if the clusters could only be formed by the much slower process of classical nucleation. For purposes of this work, interstitials were considered clustered if they were within the nearest-neighbor lattice distance of another interstitial. The size distribution of the interstitial clusters produced is a function of the cascade energy [12], and the interstitial clustering fraction is calculated by summing that distribution. Although in-cascade vacancy clustering could be treated in a similar fashion, the level of vacancy clustering is much lower over the timescale of these simulations (4).

The surviving MD defects can be conveniently described as a fraction of the NRT displacements [5] and the number of clustered interstitials as a fraction of the surviving MD defects. The energy dependence of the surviving defect fraction (η) and the interstitial clustering fraction (f_{icl}) from the MD simulations is shown in Figs. 1 and 2, respectively. Because the dependence of the results on the irradiation temperature was weak, all of the results obtained at 100, 600, and 900 K are shown in Refs. [2,3,12]. The line drawn through the data in each figure is a nonlinear least squares fit to the data using the following functions:

$$\eta = 0.5608 E_{MD}^{(-0.3029)} + 3.227 \times 10^{-3} E_{MD}, \quad (1)$$

$$f_{icl} = [0.097 \ln(E_{MD} + 0.9)]^{0.3859} - 7 \times 10^{-6} E_{MD}^{2.5}, \quad (2)$$

where E_{MD} is in keV. Interstitial clustering can also be expressed as a fraction of the NRT displacements by taking the product of $\eta \cdot f_{icl}$.

In both Eqs. (1) and (2), the first term in the function dominates the energy dependence up to about 20 keV. The second term is responsible for the minimum in the defect survival curve and the maximum in the interstitial clustering curve at about 20 keV. This change in the

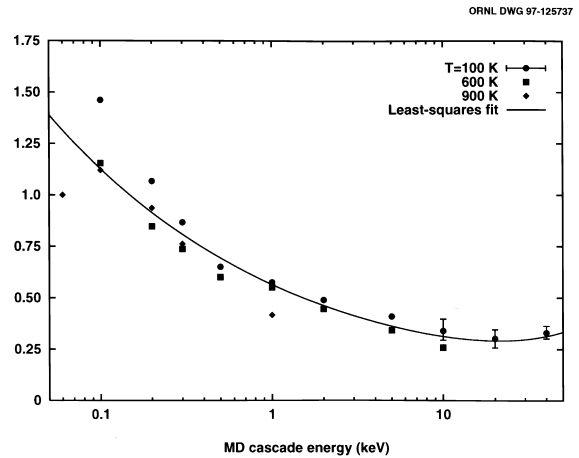


Fig. 1. Average MD point defect survival fraction as a function of cascade energy; results of MD simulations at 100, 600 and 900 K.

energy dependence occurs because subcascade formation [3,4] makes a single high-energy cascade appear to be the equivalent of several lower energy cascades. Thus, the defect survival fraction is slightly higher, and the interstitial clustering fraction slightly lower at 40 keV than at 20 keV. The increase in the defect survival fraction between 20 and 40 keV is slight, but it appears to be statistically significant from the magnitude of the standard deviations that are shown as error bars in Fig. 1. These standard deviations are based on seven cascades each at 10 and 40 keV, and ten cascades at 20 keV. Since the standard deviations on the average interstitial clustering fractions are much larger, the significance of the maximum shown in Fig. 2 is less clear.

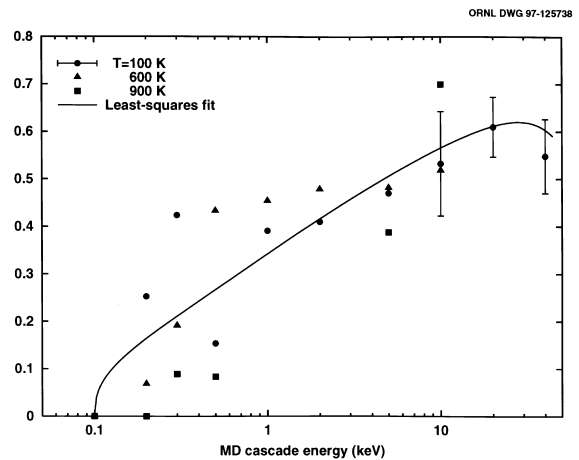


Fig. 2. Average in-cascade interstitial clustering fraction as a function of cascade energy; results of MD simulations at 100, 600 and 900 K.

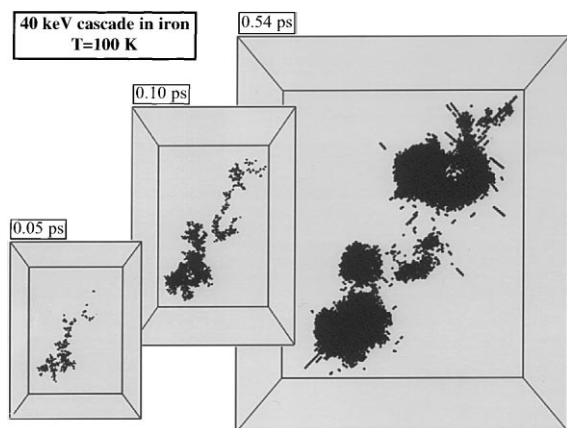


Fig. 3. Evolution of a 40 keV cascade in iron at 100 K, illustrating subcascade formation.

Based on the extensive subcascade formation observed in the 40 keV cascade simulations, it appears unlikely that η and f_{icl} will change significantly at higher cascade energies. Therefore, the values calculated from Eqs. (1) and (2) for 40 keV were applied for all the higher energy cascades in the SPECTER calculations; the values at 40 keV were: $\eta = 0.313$ and $f_{icl} = 0.603$. An example of this subcascade development in the 40 keV cascades is shown in Fig. 3.

3. Results of defect production calculations using SPECTER

Energy-dependent defect production cross sections for surviving MD defects and clustered interstitials, and spectrum-averaged values for several irradiation environments were generated by modifying the SPECOMP [6] and SPECTER [7] computer codes. SPECOMP normally calculates displacement cross sections for compounds using the primary knock-on atomic recoil energy distributions contained in a 100-neutron-energy by 100-recoil-energy grid for each of 40 different elements. For the present surviving point defect and clustered interstitial calculations, these new functions were used as a factor multiplying the standard displacement cross section equations as a function of the damage energy, T_{dam} . SPECOMP thus produced surviving defect and clustered interstitial cross sections on a 100 point neutron energy grid.

The SPECTER computer code contains libraries of calculated cross sections for displacements, gas production, and total energy distribution, as well as atomic recoil energy distributions for over 40 elements and various compounds. For a given neutron energy spectrum and irradiation time, the code will calculate the net radiation damage effects, as given above. In the present

case, the SPECOMP calculations for the surviving defect and clustered interstitial cross sections were added to the SPECTER libraries. SPECTER runs for various neutron spectra thereby produced spectrum-averaged values for the point defect and interstitial clustering fractions.

The neutron flux distributions and iron PKA spectra obtained from SPECTER for four irradiation facilities are shown in Figs. 4 and 5, respectively. The facilities illustrated are: the ITER first wall [8]; the midcore location in the Fast Flux Test Facility (FFTF) at the US DOE Hanford Reservation; the midplane of the Peripheral Target Position of the High Flux Isotope Reactor at the Oak Ridge National Laboratory (HFIR PTP); and the position one-quarter of the way through

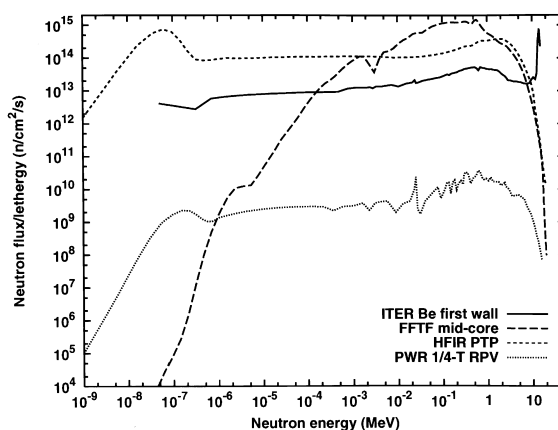


Fig. 4. Energy dependence of neutron flux in various irradiation environments: ITER (DT fusion), HFIR (light water moderated fission), FFTF (sodium moderated fission), and a commercial PWR (light water moderated fission).

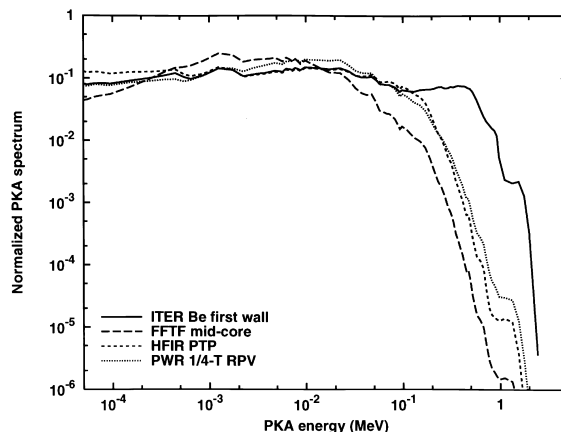


Fig. 5. Normalized iron PKA spectra from various irradiation sources: ITER (DT fusion), HFIR (light water moderated fission), FFTF (sodium moderated fission), and a commercial PWR (light water moderated fission).

the reactor pressure vessel of a typical commercial pressurized water reactor (PWR). Although the FFTF is not currently available for conducting irradiations, fusion reactor research programs have used it extensively in the past. The PKA spectra in Fig. 5 are normalized to a single neutron-PKA interaction. The differences in the neutron energy spectra in Fig. 4 arise primarily from two sources. First, differences in the neutron source term: DT fusion in the ITER and fission in the other three reactors. Secondly, differences in the neutron moderator are illustrated by comparing the sodium moderated FFTF with the light water moderated HFIR and PWR. In spite of these differences in neutron energy, the PKA energy spectra are similar. The primary distinction that can be noted among these four is the higher fraction of PKAs above ~ 0.2 MeV for the ITER spectrum. This is a result of the DT fusion neutron source term at 14.1 MeV.

4. Results of reactor comparison

The primary results of these calculations are summarized in Fig. 6. The PKA-spectrum-averaged defect survival fraction is shown in Fig. 6(a), and the interstitial clustering fraction in Fig. 6(b). In both cases, the effective production cross section has been divided by the NRT dpa cross section. In order to provide a broader comparison, values are shown for two irradiation sites in addition to those illustrated in Figs. 4 and 5. These are: a position located in the removable beryllium reflector of the HFIR (RB*), and the below-core position in the FFTF (BC).

As might be expected from Fig. 1, the average defect survival fraction shown in Fig. 6(a) decreases as the average PKA energy increases. Thus, the lowest defect survival fraction is obtained in the ITER first wall for which the average PKA energy is 48 keV as result of the 14.1 MeV neutron source term. The highest defect survival fraction occurs in the FFTF BC, where the average PKA energy is 3.4 keV. Although the FFTF was a sodium-cooled fast reactor, the average PKA energy in both FFTF sites is lower than that from any of the water-moderated fission reactor spectra, and the defect survival fraction is therefore higher. There are two reasons why the average defect survival fractions shown in Fig. 6(a) are so similar. First, the differences between the various fission and fusion PKA spectra are relatively modest in the region below about 10 keV where the energy dependence of the defect survival fraction (Fig. 1) is strongest. Then, when the PKA spectra become more different at higher energies, the defect survival fraction becomes nearly independent of energy.

The average interstitial clustering fraction (per NRT displacement) shown in Fig. 6(b) is almost independent of the initial neutron energy spectrum. Although the

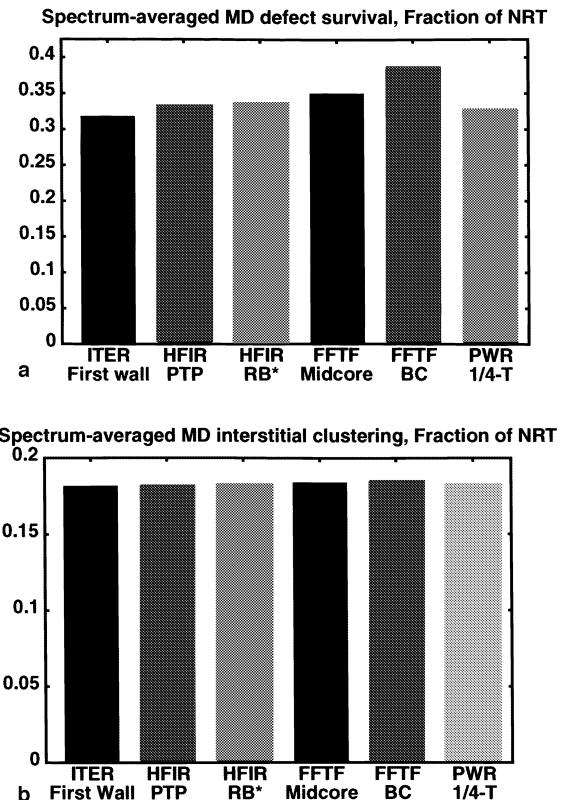


Fig. 6. Comparison of spectrally averaged damage production cross sections (per NRT dpa) for various irradiation environments; point defect survival ratio is shown in (a) and the interstitial clustering fraction is shown in (b).

average clustering fraction increases strongly with PKA energy (Fig. 2), the defect survival fraction is decreasing at a similar rate. The spectrum-averages shown in Fig. 6(b) reflect the fact that the product of Eq. (1) and Eq. (2) is nearly a constant. Overall, the values shown in Fig. 6 indicate that primary radiation damage formation in a DT fusion environment should not be significantly different from that obtained in fission reactors. The average defect survival fraction is 0.35 ± 0.03 and the interstitial clustering fraction is about 0.18 for all the cases shown.

5. Summary and discussion

Although it is not yet possible to simulate the very high energy displacement cascades that will be generated in the materials used in a DT fusion reactor first wall, examination of the MD cascade simulations in iron for energies up to 40 keV provides considerable insight. The primary damage parameters derived from the MD results exhibit a strong dependence on cascade energy up to 10 keV. This dependence is diminished and slightly

reversed between 20 and 40 keV, apparently due to the formation of well-defined subcascades in this energy region. Such an explanation is only qualitative at this time, and additional analysis of the high energy cascades is underway in an attempt to obtain a quantitative measure of the relationship between cascade morphology and defect survival. The spectrum-averaged primary damage parameters shown in Fig. 6 are only weakly dependent on the initial neutron energy spectrum. This result appears unlikely to change significantly if higher energy cascades are included in the analysis. In particular, the extensive subcascade formation observed at 40 keV suggests that the results reported here should be relevant to high-energy neutron sources such as ITER.

It should be pointed out that the MD-derived parameters reflect the primary damage state after only 10–20 ps. It would be useful to perform a similar analysis on this same set of cascades after annealing for times long enough to permit at least some vacancy diffusion. For example, this would permit a better analysis of vacancy clustering [4]. Small differences in the defect survival or interstitial cluster clustering fractions could be amplified at longer times or a stronger temperature dependence could emerge. Further work is also needed to describe the spectral dependence of the point defect cluster size distributions, not just the overall fraction clustering. However, at this time the results presented here provide the best available guidance for describing the primary damage source terms needed in the kinetic models used to simulate radiation-induced microstructural evolution.

Acknowledgements

The authors would like to thank Ed Cheng of TSI Research in Solana Beach, CA for supplying the ITER

neutron spectra and to acknowledge helpful discussions with and technical reviews by Drs S.J. Zinkle and A.F. Rowcliffe.

References

- [1] T.A. Gabriel, B.L. Bishop, F.W. Wiffen, *Nucl. Technol.* 38 (1978) 427.
- [2] R.E. Stoller, *J. Nucl. Mater.* 233–237 (1996) 999.
- [3] R.E. Stoller, *JOM* 48 (1996) 23.
- [4] R.E. Stoller, G.R. Odette, B.D. Wirth, *J. Nucl. Mater.* 251 (1997) 49.
- [5] M.J. Norgett, M.T. Robinson, I.M. Torrens, *Nucl. Eng. Des.* 33 (1975) 50.
- [6] L.R. Greenwood, in: H. Farrar IV, E.P. Lippincott (Eds.), *SPECOMP Calculations of Radiation Damage in Compounds, Reactor Dosimetry: Methods, Applications, and Standardization*, ASTM STP 1001, American Society of Testing and Materials, West Conshohocken, PA, 1989, pp. 598–602.
- [7] L.R. Greenwood, R.K. Smither, *SPECTER: Neutron Damage Calculations for Materials Irradiations*, ANL/FPP/TM-197, Argonne National Laboratory, Argonne, IL, January 1985.
- [8] G. Saji, *Activation Analysis Specification-2*, ITER San Diego JCT, August 1997.
- [9] M.W. Finnis, *MOLDY6-A Molecular Dynamics Program for Simulation of Pure Metals*, AERE R-13182, UK AEA Harwell Laboratory, 1988.
- [10] M.W. Finnis, J.E. Sinclair, *Philos. Mag. A* 50 (1984) 45; Erratum, *Philos. Mag. A* 53 (1986) 161.
- [11] A.F. Calder, D.J. Bacon, *J. Nucl. Mater.* 207 (1993) 25.
- [12] W.J. Phythian, R.E. Stoller, A.J.E. Foreman, A.F. Calder, D.J. Bacon, *J. Nucl. Mater.* 223 (1995) 245.
- [13] ASTM E521, *Standard Practice for Neutron Radiation Damage Simulation by Charged-Particle Irradiation*, Annual Book of ASTM Standards, vol. 12.02, American Society of Testing and Materials, Philadelphia.